Open access • Journal Article • DOI:10.1109/TTHZ.2020.3004517

Importance and Requirement of Frequency Band Specific RF Probes EM Models in Sub-THz and THz Measurements up to 500 GHz — Source link

Chandan Yadav, Marina Deng, Sebastien Fregonese, Marco Cabbia ...+3 more authors

Institutions: National Institute of Technology Calicut, University of Bordeaux

Published on: 23 Jun 2020 - IEEE Transactions on Terahertz Science and Technology (IEEE)

Topics: Frequency band, Radio frequency, Terahertz radiation and Radio spectrum

Related papers:

- On-Wafer Characterization of Silicon Transistors Up To 500 GHz and Analysis of Measurement Discontinuities Between the Frequency Bands
- Impact of on-Silicon De-Embedding Test Structures and RF Probes Design in the Sub-THz Range
- Importance of complete characterization setup on on-wafer TRL calibration in sub-THz range
- Comparison of On-Wafer TRL Calibration to ISS SOLT Calibration With Open-Short De-Embedding up to 500 GHz
- THz on-wafer calibration using offset-shorts and known through as standards

Share this paper:

View more about this paper here: https://typeset.io/papers/importance-and-requirement-of-frequency-band-specific-rf-1dgdkdddkj

Importance and Requirement of frequency band specific RF probes EM Models in sub-THz and THz Measurements up to 500 GHz

Chandan Yadav, Marina Deng, Sebastien Fregonese, Marco Cabbia, Magali de Matos, Bernard Plano, Thomas Zimmer

▶ **To cite this version:**

Chandan Yadav, Marina Deng, Sebastien Fregonese, Marco Cabbia, Magali de Matos, et al.. Importance and Requirement of frequency band specific RF probes EM Models in sub-THz and THz Measurements up to 500 GHz. IEEE Transactions on Terahertz Science and Technology, Institute of Electrical and Electronics Engineers, In press, pp.1-1. 10.1109/TTHZ.2020.3004517 . hal-02884144

HAL Id: hal-02884144

https://hal.archives-ouvertes.fr/hal-02884144

Submitted on 29 Jun 2020

HAL is a multi-disciplinary open access archive for the deposit and dissemination of scientific research documents, whether they are published or not. The documents may come from teaching and research institutions in France or abroad, or from public or private research centers.

L'archive ouverte pluridisciplinaire **HAL**, est destinée au dépôt et à la diffusion de documents scientifiques de niveau recherche, publiés ou non, émanant des établissements d'enseignement et de recherche français ou étrangers, des laboratoires publics ou privés.

Importance and Requirement of Frequency band specific RF probes EM Models in sub-THz and THz Measurements up to 500 GHz

Chandan Yadav, *Member, IEEE,* Marina Deng, *Member, IEEE,* Sebastien Fregonese, Marco Cabbia, Magali De Matos, Bernard Plano and Thomas Zimmer, *Senior Member, IEEE*

***Abstract*—In this paper, we present on-silicon structures on-wafer measurements up to 500 GHz and a comprehensive electromagnetic (EM) simulation analysis to understand non-ideal behaviour in the measured data. The EM simulations are performed in such a way that the simulation setup remains very close to the physical measurement environment where a faithful true EM model of the RF probes is an essential requirement. In this process, four different RF probes used during measurements in the frequency bands 1 GHz - 110 GHz, 140 GHz - 220 GHz, 220 GHz - 325 GHz and 325 GHz - 500 GHz are designed in the EM simulator. We also highlight the importance of the frequency band specific probe models to develop a deep understanding of the problems encountered in the sub-THz and THz measurements.**

***Index Terms*—On-wafer TRL calibration, test structures, thru standard, EM simulation, RF probes, SiGe HBT, sub-THz.**

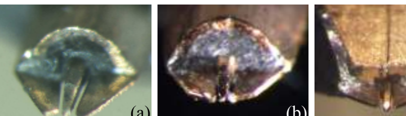
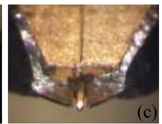
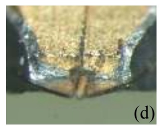

Fig. 1. Microscopic pictures of the Picoprobe RF probes used in the different measurement frequency bands: (a) 1 GHz-110 GHz, (b) 140 GHz-220 GHz, (c) 220 GHz-325 GHz and (d) 325 GHz-500 GHz.

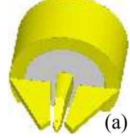

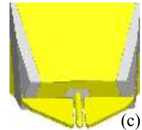
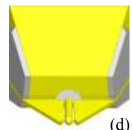

Fig. 2. Frequency band specific RF probe models corresponding to (a) 1 GHz -110 GHz, (b) 140 GHz - 220 GHz, (c) 220 GHz - 325 GHz and (d) 325 GHz - 500 GHz shown in Fig. 1. The models are designed in the HFSS and in all models, white=coaxial insulator, gray=solder, yellow=metal.

I. Introduction

FULFILLING the ever increasing demand of high-speed electronics systems for a wide range of applications e.g. communication system, imaging, radar, security etc. [1]–[4] in the sub-THz and THz ranges is very challenging. The challenges spans from high-speed semiconductor device design to system design. To design cost effective RF high speed integrated circuits for these applications, the transistors' characteristics such as the maximum available power gain frequency ($f_{\max}$) and the transconductance (g_m) plays a very important role [4], [5]. The state-of-art silicon-germanium (SiGe) HBT shows a $f_{\mathrm{T}}/f_{\max}$ of 505/720 GHz [6] and benefits from the silicon integration with an advantageous back-end-of-line (BEOL) environment compared to the III-V technology based transistors [7]. Accurate, repeatable and reliable S-parameter measurements of a transistor above 110 GHz are challenging but are urgently required to develop compact models for the high-speed RF circuit design [8]. In the sub-THz and THz ranges, the measured and calibrated S-parameters of a device can be influenced by the RF probe design, the RF pad design, the test structures design, the layout of the neighbouring structures, the substrate materials etc. along with the used calibration and de-embedding techniques [9]–[18]. A dedicated work focused on the improvement of the measurement's accuracy in sub-THz and THz ranges is necessary where an accurate and reliable simulation analysis can play a vital role.

To deepen the understanding of high frequency measurements, electromagnetic (EM) simulation is usually performed [10]–[15], [17], [19]–[21]. Out of these reported works, most of the EM simulation analyses are dedicated to test structures fabricated on non-Silicon substrate up to 110 GHz [12], [20] and above 110 GHz [10], [11], [15]. In [10], [15], the EM simulation analysis covering more than one frequency band is presented using only one RF probe model. For Si based test structures also, EM simulation analysis covering more than one frequency band (1 GHz to above 110 GHz) is presented using only one RF probe model [13], [14], [17]. In fact, the geometry and layout for each RF probe depends on the frequency band as well as on the probe head supplier. Therefore, to improve the accuracy and the reliability of the EM simulation analysis in the sub-THz and THz ranges, frequency band specific RF probe models are an essential requirement. An improvement in the on-wafer S-parameter measurement of a DUT requires a combination of an efficient on-wafer calibration kit design and the RF probe design. In order to design efficient test structures in a calibration kit, a thorough understanding of the behaviour of the test structures is required to evaluate their performance and refine them further in the next design cycle. The use of well-structured EM simulations can be one of the tools to gain insight into

Manuscript received April 16, 2019. This work is partly funded by the French Nouvelle-Aquitaine Authorities through the SUBTILE and FAST project. The authors also acknowledge financial support from the EU under Project Taranto (No. 737454). The authors would like to thank STMicroelectronics for supplying the Silicon wafer.

Marina Deng, Sebastien Fregonese, Marco Cabbia, Magali De Matos, Bernard Plano, and Thomas Zimmer are with the IMS Laboratory, University of Bordeaux France (e-mail: thomas.zimmer@ims-bordeaux.fr).

Chandan Yadav is now with the National Institute of Technology, Calicut, Kerala, 673601, India. Earlier, he was associated with the IMS laboratory, University of Bordeaux, France (e-mail: chandan@nitc.ac.in).

TABLE I

PARAMETER VALUES USED TO MODEL THE RF PROBES IN HFSS.

RF Probe Model	Pitch (μm)	min/max separation between Signal and Ground trace (μm)	Max width of ground trace in CPW (μm)	Projection Angle (degree)	Inner diameter of Coax section (μm)
1 GHz - 110 GHz	100	22.75/33	250	35	149
140 GHz - 220 GHz	50	12/24.5	230	35	130
220 GHz - 325 GHz	50	12/12	287	23	43
325 GHz - 500 GHz	50	6.5/6.5	239	22.5	45

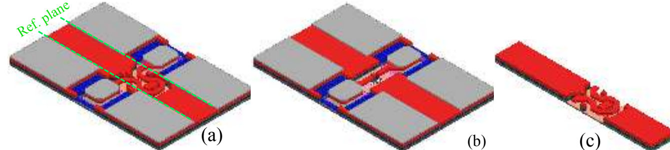

Fig. 3. 3D schematic of DUTs (a) meander line, (b) transistor open and (c) intrinsic part of the meander line. The green dashed line in (a) shows the position of the reference plane after applying the on-wafer TRL calibration.

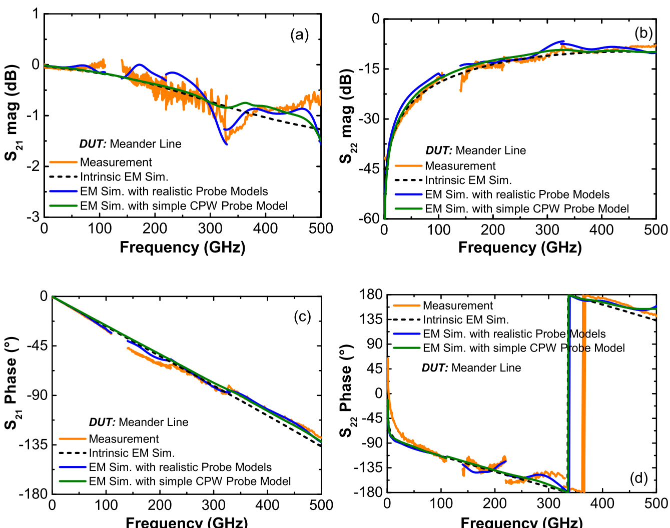

Fig. 4. S-parameter based on the measurements and EM simulation after applying the calibration on the meander line. The dashed black line is used to represent the intrinsic EM simulation. The solid blue and green lines shows predictions of RF probe models shown in Fig. 2 and Fig. 10, respectively.

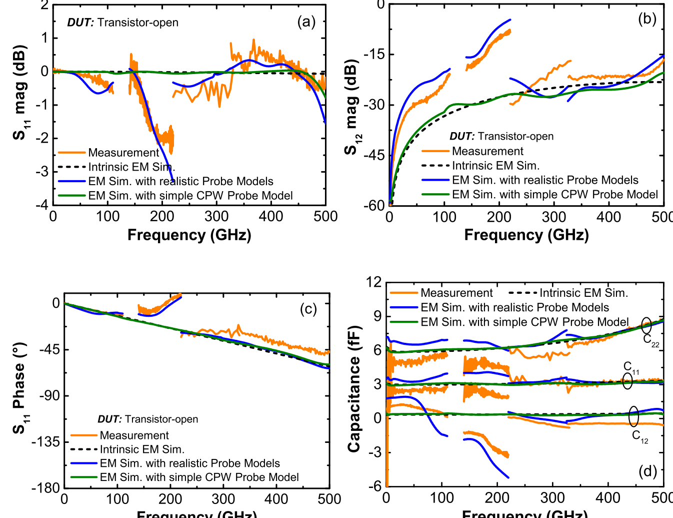

Fig. 5. S-parameter and capacitance measurements along with the EM simulation of the transistor-open up to 500 GHz. The solid blue and green lines shows predictions of RF probe models shown in Fig. 2 and Fig. 10, respectively.

the behaviour of the structures that can be used for the purpose of re-design, similarly to the use of SPICE models to optimize the circuit performance before its tape-out.

In this paper, we demonstrate the importance of well-structured EM simulations for the development of a deep understanding of the behavior of the test structures, which is essential for the re-design an optimized structures. The four frequency band specific RF probe EM models (spanning from 1 GHz to 500 GHz) are designed in HFSS and EM simulations are performed with them to thoroughly analyse the measured S-parameters' behavior of the DUTs (transistor-open and meander line). The usefulness of EM simulations for gaining deep insights into unexplored effects is highlighted. The work presented also demonstrate the use of well-structured EM simulations to understand the effects of RF probe design in high frequency measurements.

II. DESCRIPTION OF RF PROBE MODELS

To perform the on-wafer TRL calibration, the thru (35μm), the lines (115μm and 365μm) and the reflects are fabricated on the silicon substrate as well as the load to perform the impedance correction and DUTs according to the STMicroelectronics BiCMOS55 technology [22]. The on-wafer TRL calibration in the frequency range 1 GHz - 110 GHz is performed using a 365μm long line, while 115μm long line is used in the frequency range 140 GHz - 500 GHz. To measure the non-calibrated (raw) S-parameters of the on-wafer TRL calibration kit structures and DUTs, four Picoprobe probes are used in different frequency ranges: (1) 1 GHz - 110 GHz with 100 μm pitch, (2) 140 GHz - 220 GHz with 50 μm pitch, (3) 220 GHz - 325 GHz with 50 μm pitch and (4) 325 GHz - 500 GHz with 50 μm pitch. For each probe, several optical images in different orientations were captured and one picture for each probe is shown in Fig. 1. Using these pictures, a realistic model for each probe is designed in the HFSS EM simulator as shown in Fig. 2. Each probe consists of two sections, the coplanar waveguide (CPW) and the coaxial waveguide. In the HFSS RF probe models, beryllium copper (BeCu) is used as the material for the probe tips while polytetrafluoroethylene (PTFE) or teflon is used as the insulator material in the coaxial section and the characteristics impedance of the coaxial section is set to 50 Ω. The parameter values used to design the probe models are listed in Table-1. Note that all these dimensions are measured from the Picoprobes probes microscopic pictures, therefore, they may slightly differ from the exact values. The EM simulation using the band specific RF probe models is carried out similarly to the work reported in [13].

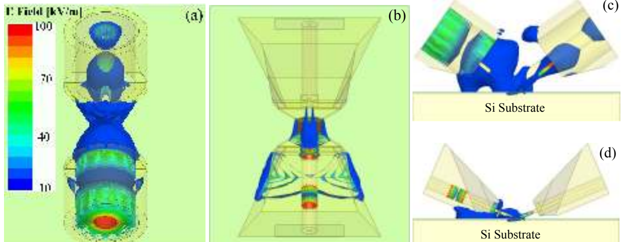

Fig. 6. Electric field (E-field) distribution (top and side views) in the transistor-open at 220 GHz using two probe models: (a, c) 1 GHz - 140 GHz and (b, d) 220 GHz – 325 GHz. The E-field distribution in all figures in this paper are shown in the same scale as shown in corner of the panel (a).

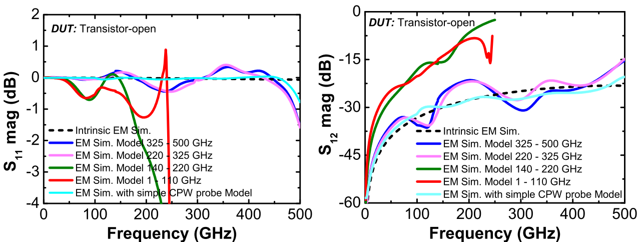

Fig. 7. Transistor-open S_{11} and S_{12} magnitude of all the four HFSS probe models compared against the intrinsic simulation. Note that the S-parameter is noisy for RF probe models 1 GHz - 110 GHz and 140 GHz - 220 GHz beyond 250 GHz and not shown to make other data easily readable.

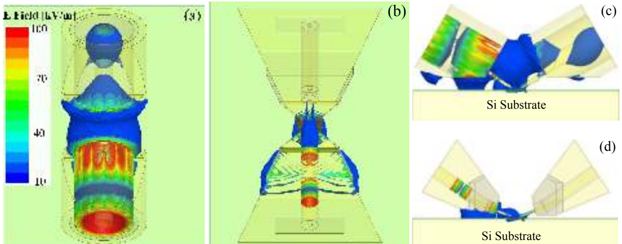

Fig. 8. E-field distribution in the transistor-open at 220 GHz using the probes designed for 140 GHz - 220 GHz ((a) and (c)) and 325 GHz – 500 GHz ((b) and (d)), where (a)-(b)= top view, (c)-(d)= side view.

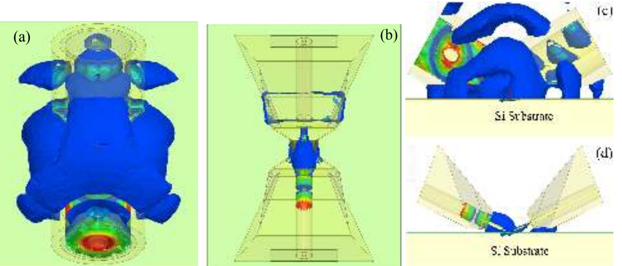

Fig. 9. E-field distribution in the transistor-open at 110 GHz using the probe model dedicated to 140 GHz - 220 GHz ((a) and (c)) and 220 GHz – 325 GHz bands((b) and (d)). (a)-(b)=top view, (c)-(d)=side view.

III. Results and Discussion

A. Measurement and EM simulation analysis of S-parameters

After measuring the non-calibrated S-parameters of the fabricated structures using the four probes mentioned in the previous section, the on-wafer TRL calibration is performed and applied to the DUTs' measurements. The on-wafer TRL calibration sets the measurement reference plane at the edge of the pad access line as shown in green color in Fig. 3a. The on-wafer TRL calibrated S-parameters of DUTs meander line and transistor-open are respectively shown in Fig. 4 and Fig. 5 with solid orange lines. When measuring the on-wafer test structures, the minimum distance between the RF probe tips at the port-1 and port-2 is $90\mu\mathrm{m}$.

To verify the accuracy and trend of the shown S-parameters, the EM simulation of the intrinsic structures of DUTs (e.g. meander line intrinsic structure in Fig. 3c) is performed where the contributions due to the RF pads and RF probes are not included. To understand the deviation of the measured data from the intrinsic EM simulation (black dashed line) in Fig. 4 and Fig. 5, an EM simulation analysis performed with a simulation setup that has an accurate representation of the physical measurement environment in the lab is beneficial. To perform such a realistic simulation, an accurate EM model of RF probes used in measurement is an essential requirement. Thus, in this work, frequency band specific EM models of RF probes as described in the previous section are used. The EM simulation of the on-wafer TRL calibration kit structures and DUTs is performed using the frequency band specific RF probe models, thereafter on-wafer TRL calibration is performed and applied on the DUTs. The resulting calibrated DUT S-parameters shown with solid blue lines in Fig. 4 and Fig. 5 are consistently following and closely matching the measured data except in 140 GHz - 220 GHz for the transistor-open which may be due to the difficulty to obtain precise measurements of a small value of S_{12}. These observations indicate that RF probe designs have a significant impact on the sub-THz and THz measurements which lead to a deviation from the ideal expected behavior predicted by intrinsic EM simulations. The frequency band specific RF probe models are very useful to deepen the understanding about various unexplored issues; two unexplored issues are discussed further. Note that all the EM simulations with the RF probe models are performed excluding neighbouring structures around the DUTs.

B. Importance of RF probe models in understanding of unexplored issue in sub-THz and THz measurement

In Fig. 4 and Fig. 5, some discontinuities in the measured data can be observed at the band edge frequencies where the RF probes are changed e.g. at 220 GHz in S_{11} and S_{12} in Fig. 5. The intrinsic EM simulation does not show any discontinuity over the entire frequency range and a similar trend is expected if only one probe model is used in the analysis [14]. Using the frequency band specific probe models in the EM simulation, the discontinuity in the measured data is correctly predicted by the EM simulation. To gain insights into this discontinuity, the E-field distributions in the transistor-open at the 220 GHz band edge are shown in Fig. 6 for the RF probe models corresponding to 1 GHz - 110 GHz and 220 GHz - 325 GHz. The E-field distribution differences show that both probes have a different influence on the DUT characteristics, which entails the discontinuity in the measured data at the band edge. In the EM simulations, the RF probes positions are similar for both probes, therefore it underlines that the discontinuity in the measurement data is not due to a misalignment of the probes [23] but it can be attributed to the combined effect of the RF probe design, the

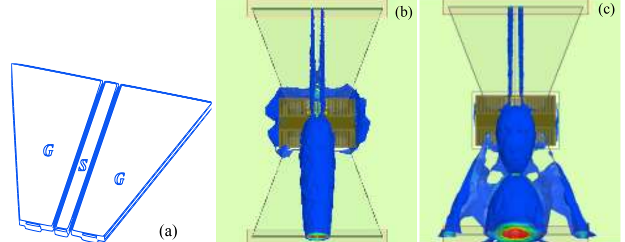

Fig. 10. E-field distribution in the transistor-open using the probe model shown at (a) 110 GHz in panel (b) and 220 GHz in panel (c). In the probe shown in (a), the signal trace width is 25μm, the ground trace minimum width is 63 μm and the metal thickness is 8.66 μm.

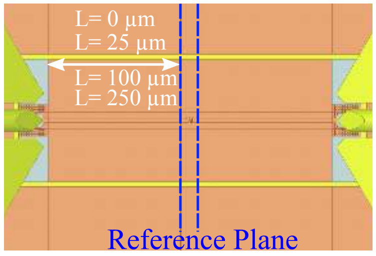

Fig. 11. The schematic of a test structure with extended access line length to study the impact of the thru length in the on-wafer TRL calibration. The access line length is extended for the DUT and for all TRL dedicated structures with "L" on each side.

calibration structure design, the distance between the probes, the calibration error etc.

In Fig. 4 and Fig. 5, another remarkable observation is the close matching of the obtained EM simulation prediction using the RF probe models of 220 GHz - 325 GHz and 325 GHz - 500 GHz with the measurements as well as with intrinsic simulation results. This clearly reflects the smaller influence of the RF probes in the measurements used in 220 GHz – 325 GHz and 325 GHz - 500 GHz. To analyze whether the smaller influence of the RF probes in the last two bands is due to the used probe design or it is independent of the RF probe design, the EM simulation predictions of each probe over the entire frequency range for the transistor-open is shown in Fig. 7. By comparing all the predictions in Fig. 7, the following observations can be made:

- RF probe models designed for 220 GHz - 325 GHz and 325 GHz - 500 GHz are consistently close to the intrinsic simulation in all bands.
- RF probe models designed for 1 GHz - 110 GHz and 140 GHz - 220 GHz are good only up to close to 220 GHz.

To obtain a better understanding about the drawn observations, the E-field distribution for each probe can be compared in Fig. 6 and Fig. 8 at 220 GHz. It can be observed that RF probes model of 1 GHz - 110 GHz and 140 GHz – 220 GHz have a higher probe-to-probe as well as a higher probe-to-substrate coupling compared to the probes model of 220 – 325 GHz and Model 325 – 500 GHz. To confirm this observation, the E-field distribution at the same scale is shown for probes (140 GHz - 220 GHz and 220 GHz - 325 GHz) at 110 GHz in Fig. 9, which confirm the findings at 220 GHz. To gain insights, the design of the RF probes is examined closely by going back again to Fig. 1 and Fig. 2. In the RF probes dedicated to the first two frequency bands (1 GHz - 110 GHz and 140 GHz - 220 GHz), the spacing between the signal and ground in the CPW section and the diameter of the dielectric ring in the coaxial section are large compared to the probes for the frequency bands (220 GHz - 325 GHz and 325 GHz - 500 GHz), see Table-1. Due to these differences in the design, the electromagnetic energy coming out of the coaxial section is more confined in the CPW section of the RF probes designed for the last two bands. Consequently, these RF probes show a lower coupling compared to the one designed for the first two frequency-bands as shown through E-field distribution in Fig. 6 to Fig. 9. To ascertain the role of the spacing between the ground and the signal trace in a RF

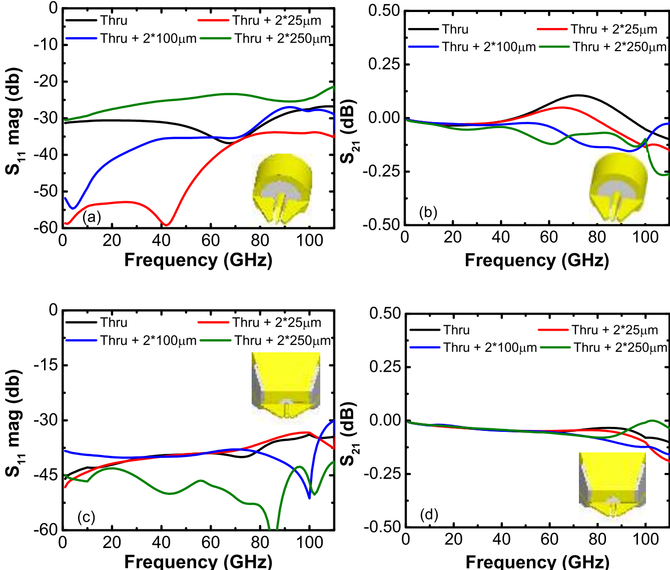

Fig. 12. S-parameter (magnitude of S_{11} and S_{21}) of a 120 μm long line using a thru with different access line lengths in the on-wafer TRL calibration. for all the cases, the reference plane is set at the same position as for the original thru. Results in panel (a) and (b) are obtained from using a RF probe corresponding to 1 GHz - 110 GHz while results of (c) and (d) are obtained using the probe corresponding to the 325 GHz - 500 GHz frequency range.

probe, a RF probe with only the CPW section as shown in Fig. 10a is designed keeping value of this separation 6.10 μm (which is less than in all the four probes). The results obtained using the CPW probe are shown in Fig. 4, Fig. 5 and Fig. 7 with "with simple CPW probe Model". The prediction of the CPW probe is very close to the intrinsic simulation and even closer than the results obtained with the RF probes designed for 220 GHz - 325 GHz and 325 GHz – 500 GHz. The E-field distribution shown for this probe in Fig. 10 indicates a lower coupling similar to the RF probes of the last two bands due to a strong energy confinement. This observation underlines that the greater confinement of the electromagnetic signal in the CPW section reduces the unwanted couplings and leads improvement in the measurement. The aforementioned EM simulation based discussion indicates that if we ignore all the involved hardware constraints and complexities, then the RF probe designs corresponding to the 220 GHz - 325 GHz and 325 GHz - 500 GHz are a better choice to be used in the frequency range 1 GHz - 220 GHz.

C. Application of the RF probe models in test structure design: A discussion on the thru length

In the design of a microstrip or co-planar based calibration kit, a thru of length of more than 400 μm to less than 100 μm was used [14], [24]–[28]. The advantage of a microstrip-based calibration kit is the elimination of the higher order modes [27]. For that reason, we adopted the microstrip-based design strategy in designing the highly scaled structures of this study. In order to clarify the impact of the thru length, we carried out an EM simulation study where we varied the access line length of the thru and naturally, all other on-wafer test structures used for on-wafer TRL calibrations as shown in Fig. 11. We placed the reference plane far away from any discontinuity (e.g. due to pad-to-access line transition and probe-to-pad transition). The access line lengths are increased by 25 μm, 100 μm and 250 μm at both port 1 and port 2. The DUT is a 120 μm long line. After applying the on-wafer TRL calibration, the obtained S-parameters are shown in Fig. 12. In general, with increase in the thru lengths in Fig. 12, S-parameters are varying as also experimentally reported in [24]. Regarding the entire frequency band in Fig. 12, no clear trend is visible; therefore, selecting the best length of thru out of all the used lengths is not obvious. Moreover, two different probe designs have been used in the investigation. A dominant effect of the thru length is expected to be independent of the probe design and bring the same amount of the variation in the S-parameter of the DUT for both probes with the same change in the thru length in Fig. 12. But Fig. 12 shows that impact of thru length variation is particular dependent on the probe design and the variation is less pronounced with the probe model corresponding to 325 GHz - 500 GHz frequency range. This behavior is appearing because an increased thru length can reduce the amount of the probe-to-probe coupling but other unwanted complex couplings that depend on the combination of the test structure and RF probe design remain present e.g. probe-to-substrate coupling. Therefore, with the use of longer test structures (i.e. longer thru) in the presented study , some improvement in measurement could have been achieved with the RF probes shown in Fig. 1, but this would have significantly increased the fabrication costs of the test structures. Thus, increasing the length of the test structure would not notably change the observations of the presented work.

IV. Conclusion

In this paper, we have demonstrated the requirements of frequency band specific EM models of RF probes for a thorough analysis of on-wafer measurements in the sub-THz and THz frequency range. Thanks to the use of RF probe models, a deep and clear understanding is presented of two unexplored effects that occur in the on-wafer measurement data of the transistor-open. Using different RF probe designs in the EM simulation, we have highlighted that the amount of the unwanted couplings varies with the RF probes design for a given test structure design, and the reduction of the unwanted coupling leads to an improvement in the on-wafer measurements. High frequency measurements can be improved by the correct design of RF probes, and test structures and the use of well-structured EM simulations can be one of the tools to gain insight on into the behavior of structures that can be used for re-design the purposes.

References

[1] J. Lee *et al.*, "Spectrum for 5G: Global Status, Challenges, and Enabling Technologies," *IEEE Commun. Mag.*, vol. 56, no. 3, pp. 12–18, March 2018. doi: 10.1109/MCOM.2018.1700818

[2] J. Grzyb, K. Statnikov, N. Sarmah, B. Heinemann, and U. R. Pfeiffer, "A 210–270-GHz Circularly Polarized FMCW Radar With a Single-Lens-Coupled SiGe HBT Chip," *IEEE Trans. THz Sci. Technol.*, vol. 6, no. 6, pp. 771–783, Nov 2016. doi: 10.1109/TTHZ.2016.2602539

[3] K. Sengupta, D. Seo, L. Yang, and A. Hajimiri, "Silicon Integrated 280 GHz Imaging Chipset With 4×4 SiGe Receiver Array and CMOS Source," *IEEE Trans. THz Sci. Technol.*, vol. 5, no. 3, pp. 427–437, May 2015. doi: 10.1109/TTHZ.2015.2414826

[4] E. Seok *et al.*, "A 410GHz CMOS Push-Push Oscillator with an On-Chip Patch Antenna," in *IEEE Int. Solid-State Circuits Conf. - Dig. Tech. Papers*, Feb 2008. doi: 10.1109/ISSCC.2008.4523262 pp. 472–629.

[5] S. Kong, C. Kim, and S. Hong, "A K-Band UWB Low-Noise CMOS Mixer With Bleeding PathG_m-Boosting Technique," *IEEE Trans. Circuits Syst. II, Exp. Briefs*, vol. 60, no. 3, pp. 117–121, March 2013. doi: 10.1109/TCSII.2013.2240792

[6] B. Heinemann *et al.*, "SiGe HBT with f_x/f_{max} of 505 GHz/720 GHz," in *Proc. IEEE Int. Electron Devices Meeting (IEDM)*, Dec. 2016, pp. 3.1.1–3.1.4, doi=10.1109/IEDM.2016.7838335.

[7] P. Chevalier *et al.*, "Si/SiGe:C and InP/GaAsSb Heterojunction Bipolar Transistors for THz Applications," *Proceedings of the IEEE*, vol. 105, no. 6, pp. 1035–1050, June 2017. doi: 10.1109/JPROC.2017.2669087

[8] B. Ardouin *et al.*, "Compact Model Validation Strategies Based on Dedicated and Benchmark Circuit Blocks for the mm-Wave Frequency Range," in *IEEE Compound Semiconductor Integrated Circuit Symposium (CSICS)*, Oct. 2015. doi: 10.1109/CSICS.2015.7314492 pp. 1–4.

[9] C. Yadav *et al.*, "Importance of complete characterization setup on on-wafer TRL calibration in sub-THz range," in *IEEE Int. Conference on Microelectronic Test Structures (ICMTS)*, March 2018, pp. 197–201, doi:10.1109/ICMTS.2018.8383798.

[10] M. S. Eggebert *et al.*, "On the Accurate Measurement and Calibration of S-parameters for Milimeter Wavelenths and Beyond," *IEEE Trans. Microw. Theory Techn.*, vol. 63, no. 7, pp. 2335 – 2342, July 2015. doi: 10.1109/TMTT.2015.2436919

[11] D. Müller *et al.*, "Impact of Ground Via Placement in On-Wafer Contact Pad Design up to 325 GHz," *IEEE Trans. Compon. Packag. Manuf. Technol.*, vol. 8, no. 8, pp. 1440–1450, Aug 2018. doi: 10.1109/TCPMT.2018.2811482

[12] G. N. Phung *et al.*, "Influence of Microwave Probes on Calibrated On-Wafer Measurements," *IEEE Trans. Microw. Theory Techn.*, vol. 67, no. 5, pp. 1892–1900, May 2019. doi: 10.1109/TMTT.2019.2903400

[13] C. Yadav *et al.*, "Impact of on-Silicon de-embedding test structures and RF probes design in the Sub-THz range," in 48th *European Microwave Conference (EuMC)*, Sept. 2018, pp. 21 – 24, Madrid, Spain.

[14] S. Fregonese *et al.*, "On-Wafer Characterization of Silicon Transistors Up To 500 GHz and Analysis of Measurement Discontinuities Between the Frequency Bands," *IEEE Trans. Microw. Theory Techn.*, vol. 66, no. 7, pp. 3332–3341, July 2018. doi: 10.1109/TMTT.2018.2832067

[15] M. Spirito, C. De Martino, and L. Galatro, "On the Impact of Radiation Losses in TRL Calibrations," in 91st *ARFTG Microwave Measurement Conference*, June 2018. doi: 10.1109/ARFTG.2018.8423820 pp. 1–3.

[16] M. Deng *et al.*, "Benefits and validation of 4-dummies de-embedding method for characterization of SiGe HBT in G-band," in *2013 European Microwave Integrated Circuit Conference*, Oct 2013, pp. 388–391.

[17] S. Fregonese *et al.*, "Comparision of On-Wafer TRL Calibration to ISS SOLT Calibration with Open-Short De-embedding up to 500 GHz," *IEEE Trans. THz Sci. Technol.*, vol. 9, no. 1, pp. 89–97, Jan. 2019. doi: 10.1109/TTHZ.2018.2884612

[18] M. Deng *et al.*, "RF Characterization of 28 nm FD-SOI Transistors Up To 220 GHz ," in *Joint Int. EUROSOI Workshop and Int. Conf. on Ultimate Integration on Silicon (EUROSOI-ULIS)*, Apr 2019.

[19] C. Andrei *et al.*, "Coupling on-wafer measurement errors and their impact on calibration and de-embedding up to 110 GHz for CMOS millimeter wave characterizations," in *2007 IEEE Int. Conference on Microelectronic Test Structures*, March 2007. doi: 10.1109/ICMTS.2007.374494 pp. 253–256.

[20] D. F. Williams *et al.*, “Crosstalk Corrections for Coplanar-Waveguide Scattering-Parameter Calibrations,” *IEEE Trans. Microw. Theory Techn.*, vol. 62, no. 8, pp. 1748 – 1761, Aug. 2014. doi: 10.1109/TMTT.2014.2331623

[21] T. J. Reck *et al.*, “Micromachined Probes for Submillimeter-Wave On-Wafer Measurements—Part II: RF Design and Characterization,” *IEEE Trans. THz Sci. Technol.*, vol. 1, no. 2, pp. 357–363, Nov 2011. doi: 10.1109/TTHZ.2011.2165020

[22] P. Chevalier *et al.*, “A 55 nm triple gate oxide 9 metal layers SiGe BiCMOS technology featuring 320 GHz f_T/ 370 GHz f_{MAX} HBT and high-Q millimeter-wave passives,” in *Proc. IEEE Int. Electron Devices Meeting (IEDM)*, Dec. 2014, pp. 3.9.1–3.9.3, doi=10.1109/IEDM.2014.7046978.

[23] C. B. Sia, “Minimizing discontinuities in wafer-level sub-THz measurements up to 750 GHz for device modelling applications,” in 89th *ARFTG Microwave Measurement Conference (ARFTG)*, June 2017. doi: 10.1109/ARFTG.2017.8000843 pp. 1–4.

[24] A. Orii, M. Suizu, S. Amakawa, K. Katayama, K. Takano, M. Motoyoshi, T. Yoshida, and M. Fujishima, “On the length of THRU standard for TRL de-embedding on Si substrate above 110 GHz,” in *2013 IEEE International Conference on Microelectronic Test Structures (ICMTS)*, March 2013. doi: 10.1109/ICMTS.2013.6528150 pp. 81–86.

[25] S. Amakawa, A. Orii, K. Katayama, K. Takano, M. Motoyoshi, T. Yoshida, and M. Fujishima, “Design of well-behaved low-loss Millimetre-Wave CMOS Transmission Lines,” in *2014 IEEE 18th Workshop on Signal and Power Integrity (SPI)*, May 2014. doi: 10.1109/SaPIW.2014.6844526 pp. 1–4.

[26] L. Galatro, A. Pawlak, M. Schroter, and M. Spirito, “Capacitively Loaded Inverted CPWs for Distributed TRL-Based De-Embedding at (Sub) mm-Waves,” *IEEE Trans. Microw. Theory Techn.*, vol. 65, no. 12, pp. 4914–4924, Dec 2017. doi: 10.1109/TMTT.2017.2727498

[27] D. F. Williams, A. C. Young, and M. Urteaga, “A Prescription for Sub-Millimeter-Wave Transistor Characterization,” *IEEE Trans. THz Sci. Technol.*, vol. 3, no. 4, pp. 433–439, July 2013. doi: 10.1109/TTHZ.2013.2255332

[28] K. H. K. Yau, I. Sarkas, A. Tomkins, P. Chevalier, and S. P. Voinigescu, “On-wafer S-parameter de-embedding of Silicon Active and Passive Devices up to 170 GHz,” in *2010 IEEE MTT-S International Microwave Symposium*, May 2010. doi: 10.1109/MWSYM.2010.5518218 pp. 600–603.